CHIN. PHYS. LETT. Vol. 36, No. 6 (2019) 067801

Nonlinear Optical Rectification, Second and Third Harmonic Generations in Square-Step and Graded-Step Quantum Wells under Intense Laser Field

O. Ozturk[1], E. Ozturk[2**], S. Elagoz[3]

[1]*Department of Nanotechnology Engineering, Cumhuriyet University, Sivas 58140, Turkey*
[2]*Department of Physics, Cumhuriyet University, Sivas 58140, Turkey*
[3]*ASELSAN-Microelectronics, Guidance & Electro-Optics, Ankara, Turkey*

(Received 20 February 2019)

For square-step quantum wells (SSQWs) and graded-step quantum wells (GSQWs), the nonlinear optical rectification (NOR), second harmonic generation (SHG) and third harmonic generation (THG) coefficients under an intense laser field (ILF) are analyzed. The found results indicate that ILF can ensure a vital influence on the shape and height of the confined potential profile of both SSQWs and GSQWs, and alterations of the dipole moment matrix elements and the energy levels are adhered on the profile of the confined potential. According to the results, the potential profile and height of the GSQWs are affected more significantly by ILF intensity compared to SSQWs. These results indicate that NOR, SHG and THG coefficients of SSQWs and GSQWs may be calibrated in a preferred energy range and the magnitude of the resonance peak (RP) by tuning the ILF parameter. It is feasible to classify blue or red shifts in RP locations of NOR, SHG and THG coefficients by varying the ILF parameter. Our results can be useful in investigating new ways of manipulating the opto-electronic properties of semiconductor QW devices.

PACS: 78.67.De, 73.90.+f, 73.21.Fg DOI: 10.1088/0256-307X/36/6/067801

The rapid progress in semiconductor growth techniques such as molecular beam epitaxy (MBE) and metal organic chemical vapor deposition (MOCVD) has accelerated research in low-dimensional semiconductor (LDS) hetero-structures due to their intrinsic physical properties and technological applications in electronic and optoelectronic devices, such as the semiconductor lasers, single-electron transistors, quantum computing, photo-detectors and high-speed electro-optical modulators. In basic physics, LDS hetero-structures create a new field of research and proposal of an extensive range of potential implementations for opto-electronic devices.[1,2] The electronic properties of these LDS hetero-structures also vary greatly depending on the entity of some asymmetry of the potential profile. This kind of an asymmetry in potential shape may be acquired either by regularly grading quantum well (QW) or applying an electric field to a symmetric QW. The differently shaped QWs[3,4] such as square QWs[5–8] and graded QWs[9,10] are well known. By altering the QW potential shape, both the energy levels (ELs) and their wave-functions modify, and numerous physical characteristics modify suitably. It has acquired rising emphasis due to numerous applications, including highly non-homogeneous parts. These structures offer the preferred optical and electronic characteristics for device projects that may be used to modulate and control the output of semiconductor devices.

Linear and nonlinear optical characteristics have been considered expansively in LDS structures because of the device application potentials in the infrared region of the electromagnetic spectrum. These optical operations in intersubband (ISB) transitions highlighted the possibility of causing small energy separation between state levels, great dipole moment matrix element (DMME) values and the possibility of resonance conditions due to the strong quantum limiting effect. These DMMEs are a clear indication that semiconductor QW structures have large nonlinearity. Experimental observations of linear and nonlinear optical properties, associated with IBS transitions, in LDSs have been reported,[11–13] and applications based on quantum hetero-structures have been investigated.[14–16] The experimental use of these devices in lasers, infrared detectors, optical amplifiers, surface light emitters, light emitter diodes, and other optoelectronic devices are displayed. The investigations of second and third order nonlinearities are crucial for nonlinear optical features of LDSs. Later, researchers studied nonlinear optical rectification (NOR), second harmonic generation (SHG) and third harmonic generation (THG) coefficients in LDSs.[17–24] They derived that high-order nonlinear optical effects are very sensible to LDSs.

The effects on the limiting potential of intense laser field (ILF) play a considerable role in the opto-electronic device model. When the confined potential of the system is significantly changed, the optical characteristics as well as bound state ELs are importantly affected. As is known, a high frequency ILF effect can cause large variations in the confined potential of

**Corresponding author. Email: eozturk@cumhuriyet.edu.tr
© 2019 Chinese Physical Society and IOP Publishing Ltd

QW constructions.[24–26] Lima *et al.*[27] have examined the transition from single to double QW potential by induced ILF. Their results display that rapid estimation of excited levels for GaAs/GaAlAs QWs with increased ILF values indicates the possibility of increased population inversion to the optical pumping scheme, which is attractive for the project of powerful QW lasers. Consequently, we consider that it is significant to examine the influence of ILF on the nonlinear optical characteristics for different QW structures.

Different quantum well growing techniques, with spatial dependence on the aluminum concentration, have been performed by several researchers.[28–31] One of these techniques can be used to obtain a large number of semiconducting devices with graded profiles. We are interested in studying $Ga_{1-x}Al_xAs/GaAs$ structures of square-step quantum wells (SSQWs) and graded-step quantum wells (GSQWs), different from the literature.[24,32,33] Because GaAlAs/GaAs QW samples are useful in modern photo-electronics and high-speed electronic devices, the pressure and external field additions of the electrical and optical characteristics in the connected systems have been considered widely.[34–38] This study focuses on the theoretical work of NOR, SHG and THG coefficients depending on ILF intensity in SSQWs and GSQWs. According to our knowledge, there is no study on comparing these nonlinear optical characteristics in SSQW and GSQW structures.

In the effective-mass approach, the wavefunctions and the state ELs for electrons in SSQWs and GSQWs, which are enlarged along the z-axis, may be achieved by dissolving the one-dimensional Schrödinger equation with a suitable Hamiltonian,

$$\Big(-\frac{\hbar^2}{2m^*}\frac{d^2}{dz^2}+V(z)\Big)\Psi(z)=E\Psi(z), \tag{1}$$

where $V(z)$ is the confined potential, and E and $\Psi(z)$ are the eigen-energy and eigen-function of the solution to Eq. (1). The confinement potentials of SSQWs and GSQWs, $L_{\rm L}$, $L_{\rm M}$, $L_{\rm R}$ being the left, middle, and right well widths, respectively, are taken as

$$V^{\rm SSQW}(z)=\begin{cases}V_1+\frac{V_2}{2}, & -(L_{\rm L}+\frac{L_{\rm M}}{2})\leqslant z\leqslant -(\frac{L_{\rm M}}{2}),\\ \frac{V_2}{2}, & -\frac{L_{\rm M}}{2}\leqslant z\leqslant \frac{L_{\rm M}}{2},\\ 0, & \frac{L_{\rm M}}{2}\leqslant z\leqslant (\frac{L_{\rm M}}{2}+L_{\rm R}),\\ V_3, & \text{elsewhere.}\end{cases} \tag{2a}$$

$$V^{\rm GSQW}(z)=\begin{cases}\frac{1}{L_{\rm L}}(z+(\frac{L_{\rm M}}{2}+L_{\rm L}))V_1+(V_1+\frac{V_2}{2}),\\ \qquad -(L_{\rm L}+\frac{L_{\rm M}}{2})\leqslant z\leqslant -(\frac{L_{\rm M}}{2}),\\ \frac{z}{2L_{\rm M}}V_2+(\frac{V_1+V_2}{2}), \quad -\frac{L_{\rm M}}{2}\leqslant z\leqslant \frac{L_{\rm M}}{2},\\ \frac{1}{L_{\rm R}}(z-(\frac{L_{\rm M}}{2}+L_{\rm R}))\frac{V_3}{3}+(\frac{V_3}{3}),\\ \qquad \frac{L_{\rm M}}{2}\leqslant z\leqslant (\frac{L_{\rm M}}{2}+L_{\rm R}),\\ V_3, \ \text{elsewhere.}\end{cases} \tag{2b}$$

Discontinuity on the side of the conduction band for both structures is analyzed using

$$V_i=\%60(1.155x_i+0.37x_i^2)\,(\text{eV}),\ (i=1,2,3). \tag{3}$$

Looking to adjoin the non-resonant polarized ILF actions throughout the z-direction, the Floquet method has been traced.[39] In the high frequency regime,[40,41] a closed-form term for the dressed potential is exhibited. Therefore, the second term on the left-hand side of Eq. (1) can be modified by $V(z)\to\langle V(z,\alpha_0)\rangle$. The laser-dressed potentials are offered by[40]

$$\langle V(z,\alpha_0)\rangle=\frac{\Omega}{2\pi}\int_0^{2\pi/\Omega}V[z+\alpha_0\sin(\Omega t)]dt, \tag{4}$$

where $\alpha_0=\sqrt{\frac{e^2 8\pi I_{\rm laser}}{m^{*2}c\Omega^4}}$ is the laser-dressing parameter,[33,42] c is the speed of light in vacuum, Ω is the laser frequency, and $I_{\rm laser}$ is the mean intensity of the laser.

After the wavefunctions and eigen-energies are achieved, the NOR,[22,23] SHG[21,22] and THG[21,22] coefficients under the compact density matrix approach can be given by

$$\begin{aligned}\chi_0^{(2)}=&\frac{4e^3\sigma_{\rm v}}{\varepsilon_0}M_{21}^2\delta_{21}\Big[E_{21}^2\Big(1+\frac{\Gamma_2}{\Gamma_1}\Big)+\hbar^2(\omega^2\\ &+\Gamma_2^2)\Big(\frac{\Gamma_2}{\Gamma_1}-1\Big)\Big]\Big/[((E_{21}-\hbar\omega)^2\\ &+(\hbar\Gamma_2)^2)((E_{21}+\hbar\omega)^2+(\hbar\Gamma_2)^2)],\end{aligned} \tag{5}$$

$$\begin{aligned}\chi_{2\omega}^{(2)}=&\frac{e^3\sigma_{\rm v}}{\varepsilon_0}[M_{21}M_{32}M_{31}]/[(\hbar\omega-E_{21}\\ &-i\hbar\Gamma_3)(2\hbar\omega-E_{31}-i\hbar\Gamma_3/2)],\end{aligned} \tag{6}$$

$$\begin{aligned}\chi_{3\omega}^{(3)}=&\frac{e^4\sigma_{\rm v}}{\varepsilon_0}[M_{21}M_{32}M_{43}M_{41}]/[(\hbar\omega-E_{21}\\ &-i\hbar\Gamma_3)(2\hbar\omega-E_{31}-i\hbar\Gamma_3/2)(3\hbar\omega\\ &-E_{41}-i\hbar\Gamma_3/3)],\end{aligned} \tag{7}$$

with ISB DMMEs being defined by

$$M_{fi}=\int\Psi_f^*z\Psi_i dz,\quad (i,f=1,2,3,4), \tag{8}$$

where ω is the angular frequency of the incident photon, $E_{fi}=E_f-E_i=\hbar\omega_{fi}$, E_i and E_f symbolize the quantized ELs for the initial and final states, respectively, the intra-subband DMME is $\delta_{21}=M_{22}-M_{11}$, $\sigma_{\rm v}$ is the carrier density, and ε_0 is the vacuum permittivity.

We have theoretically analyzed the NOR, SHG and THG coefficients in SSQWs and GSQWs under an ILF. Herein, all well widths are $L=L_{\rm L}=L_{\rm M}=L_{\rm R}=10\,\text{nm}$, $x_1=0.1$, $x_2=0.2$, $x_3=0.3$, $T_1=1/\Gamma_1=1\,\text{ps}$ $T_2=1/\Gamma_2=0.2\,\text{ps}$, $T_3=1/\Gamma_3=0.5\,\text{ps}$, and $\sigma_{\rm v}=3\times10^{22}\,\text{m}^{-3}$.

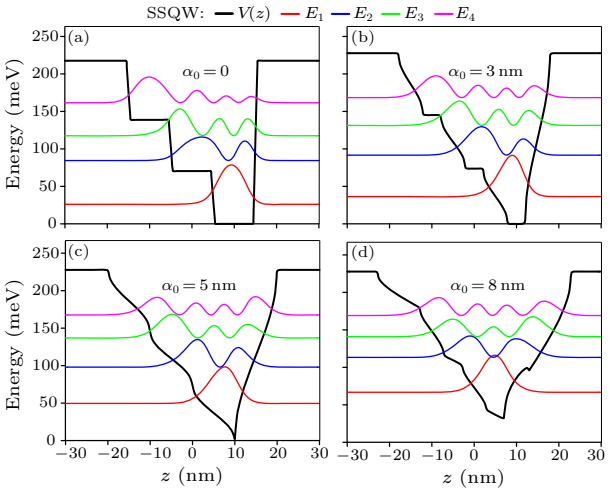

Fig. 1. The confined potential (black curve) and squared wave functions related to the first four energy states for the SSQWs: (a) $\alpha_0 = 0$, (b) $\alpha_0 = 3\,\text{nm}$, (c) $\alpha_0 = 5\,\text{nm}$, and (d) $\alpha_0 = 8\,\text{nm}$.

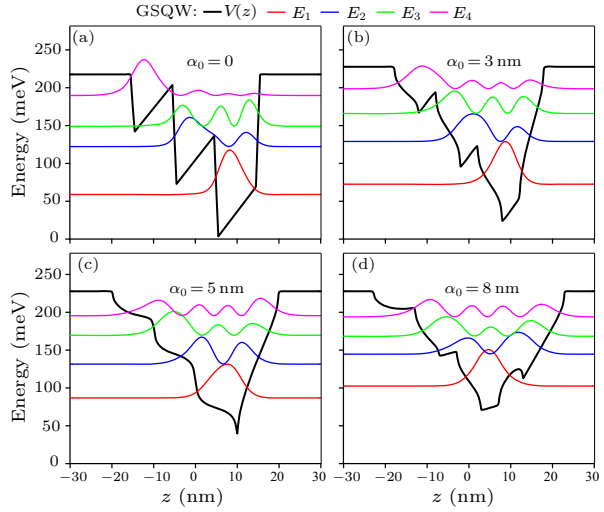

Fig. 2. The confined potential (black curve) and squared wave functions related to the first four energy states for the GSQW: (a) $\alpha_0 = 0$, (b) $\alpha_0 = 3\,\text{nm}$, (c) $\alpha_0 = 5\,\text{nm}$, and (d) $\alpha_0 = 8\,\text{nm}$.

For different ILF values, the confined potential and the squared wavefunctions related to the first four energy states of SSQWs and GSQWs are shown in Figs. 1 and 2. As expected, by increasing ILF, the width, height and shape of the effective well, ELs and the electron probability densities in SSQW and GSQW have changed importantly. We have seen from these figures that the potential profile and height of the GSQW are more affected by the ILF. When the ILF is present, the bottom of the potential in the GSQW changes upwards, whereas this change in SSQW occurs at $\alpha_0 > L/2$. By increasing ILF ($\alpha_0 > L/2$), all potential shapes completely change, the depths of the confined potential decrease. With and without the ILF, here the ELs in the SSQW are smaller than those in the GSQW. For example, for $\alpha_0 = 0$ ($\alpha_0 = 5\,\text{nm}$) ELs of the SSQW are 26, 84, 117 and 161 meV (49, 98, 136 and 167 meV), respectively, whereas ELs of GSQW are 58, 122, 149 and 189 meV (86, 131, 169 and 195 meV), respectively. As can be seen from both the figures, the largest change is seen in the ground state energy with the effect of ILF and the smallest change is in the fourth energy state. In the case of ILF, we obtain that the analyzed alteration in the confined potential and ELs will importantly influence the nonlinear optical characteristics of the structure based on ISB transitions.

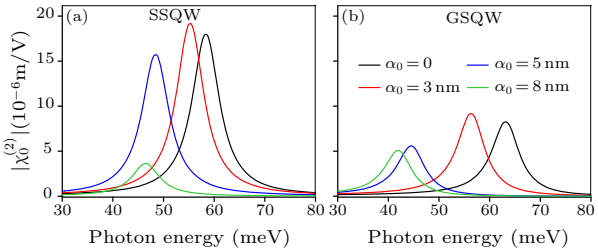

Fig. 3. The NOR coefficient versus photon energy for different ILF values for (a) SSQW and (b) GSQW.

For the SSQW and GSQW, Figs. 3(a) and 3(b) present the calculated NOR coefficient versus the photon energy under an ILF. The shift of NOR coefficient is attributed to the change of E_{21} with the increase of ILF. We can see that the spectrum shows a red shift, which is related to the decrease of E_{21} with the increase of the ILF. The position of the resonant peak (RP) is at $E_{21} \approx \hbar\omega$, thus the shift of RP should be consistent with the change of energy interval E_{21}. The change of the amplitude of RPs of NOR coefficient is consistent with the change of DMMEs $|M_{21}^2\delta_{21}|$. The non-zero values of ($|\delta_{21}|$) contributing in the magnitude of NOR is attributed to the presence of asymmetry in potential profile. The intra-subband DMME $|\delta_{21}|$ is the minimum at $\alpha_0 = 9\,\text{nm}$ and $\alpha_0 = 6\,\text{nm}$ for SSQW and GSQW, respectively (see Fig. 6(b)). As seen in Fig. 3, for both the SSQW and GSQW, the magnitude of the NOR coefficient is the maximum at $\alpha_0 = 3\,\text{nm}$ and the minimum at $\alpha_0 = 8\,\text{nm}$.

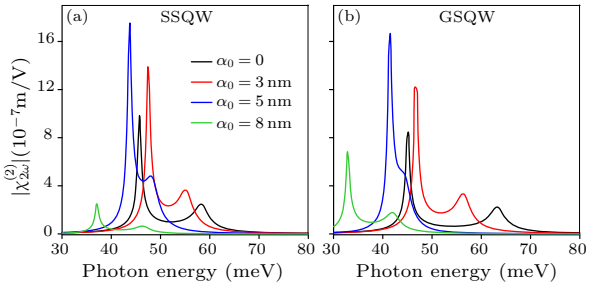

Fig. 4. The SHG coefficient versus the photon energy for different ILF values for (a) SSQW and (b) GSQW.

For different ILF values, SHG coefficients versus the photon energy for the SSQW and GSQW are displayed in Figs. 4(a) and 4(b). There are two RPs corresponding to each of the resonance frequencies. The corresponding position of RP is at $E_{31}/2 \approx \hbar\omega$

(dominant-major peak) and at $E_{21} \approx \hbar\omega$ (weak-minor peak). The energy difference between the two peaks is listed in Table 1. The separation of the SHG signal results directly from the asymmetrically spaced ELs. We can see that the blue-shift or red-shift is not the same for each of the RPs. The value of $E_{31}/2$ increases up to $\alpha_0 \leqslant 3\,\text{nm}$ while it decreases for $\alpha_0 > 3\,\text{nm}$. Thus the dominant peak shows the blue-shift up to $\alpha_0 \leqslant 3\,\text{nm}$ and the red-shift for $\alpha_0 > 3\,\text{nm}$. The value of E_{21} increases for $0 < \alpha_0 \leqslant 1\,\text{nm}$ and then decreases for $\alpha_0 > 1\,\text{nm}$. The weak peak indicates the red-shift relative to rising ILF parameters in this figure. As the ILF value increases, the energy differences in GSQW vary more than in SSQW (see Fig. 6(a)). The magnitude of RPs of SHG coefficient is consistent with the variations of the absolute DMMEs $|M_{21}M_{32}M_{31}|$ and the energy differences. The physical cause behind these consequences is the variation in the electron confinement induced by the changes of ILF parameters. Because the GSQW is more affected by the increase of ILF, the largest difference between GSQW and SSQW for the magnitude of SHG coefficient is at $\alpha_0 = 8\,\text{nm}$.

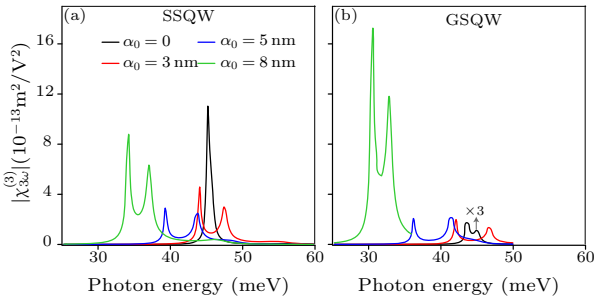

Fig. 5. The THG coefficient versus the photon energy with different ILF values for (a) SSQW and (b) GSQW. The black curve for GSQW in (b) has been multiplied by 3.

Table 1. For SSQW and GSQW, the energy differences between the resonant peaks for different ILF values.

α_0 (nm)	SSQW Energy difference (meV)			GSQW Energy difference (meV)		
	$E_{21}-\frac{1}{2}E_{31}$	$\frac{1}{2}E_{31}-\frac{1}{3}E_{41}$	$E_{21}-\frac{1}{3}E_{41}$	$E_{21}-\frac{1}{2}E_{31}$	$\frac{1}{2}E_{31}-\frac{1}{3}E_{41}$	$E_{21}-\frac{1}{3}E_{41}$
0	12.65	0.55	13.21	18.22	1.45	19.68
3	7.78	3.48	11.26	9.76	4.68	14.45
5	4.77	4.34	9.11	3.30	5.15	8.45
8	9.40	2.97	12.38	9.23	2.42	11.66

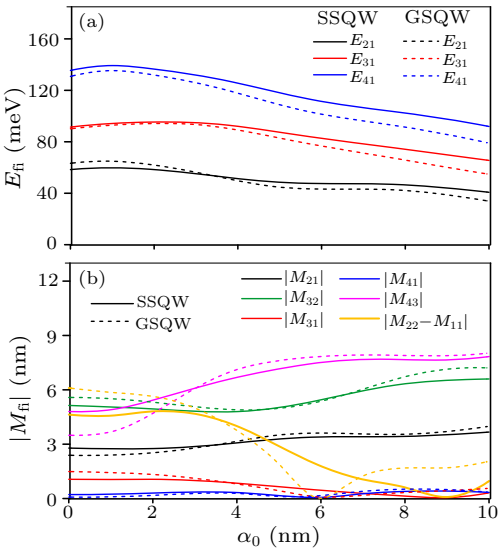

Fig. 6. (a) Several energy differences and (b) several dipole matrix elements as a function of ILF for SSQW and GSQW.

The THG coefficient as a function of the photon energy for different ILF values is given in Figs. 5(a) and 5(b) for the SSQW and GSQW, respectively. In this figure, it can be seen that there are three resonance peaks corresponding to each of the resonance frequencies. The coincident location of RP is at $E_{41}/3 \approx \hbar\omega$ (dominant-major peak), $E_{31}/2 \approx \hbar\omega$ (middle peak) and at $E_{21} \approx \hbar\omega$ (very weak-minor peak). The energy differences among the three peaks are also listed in Table 1. It is obvious that the energy differences of SSQW and GSQW are different from each other. The value of $E_{41/3}$ increases for $0 < \alpha_0 \leqslant 1\,\text{nm}$ and then decreases for $\alpha_0 > 1\,\text{nm}$ (see Fig. 6(a)), thus the dominant peak shows the red-shift relative to the increase of ILF parameters. The variations of $E_{31}/2$ and E_{21} are as in the SHG coefficient. The results show that the changes of RP size of THG are directly related, not only to the absolute DMMEs $|M_{21}M_{32}M_{43}M_{41}|$, but also to the energy interval $E_{21}E_{31}E_{41}$ in the denominator by introducing more asymmetry into the system. For the size of the THG coefficient, the most significant differences between GSQW and SSQW are at $\alpha_0 = 0$ and $\alpha_0 = 8\,\text{nm}$. As seen from Fig. 6(b), the minimum and maximum of DMMEs depend on the ILF parameter. Such a dependence of the energy differences and DMMEs on ILF intensity can be valuable for varied potential device applications.

As a result, ILF values are very effective on NOR, SHG and THG coefficients in both SSQW and GSQW systems. Since the potential well shape is modified with rising ILF, the ELs, the electron probability densities and the dipole matrix elements vary, and this process could be utilized as a method to examine the limitation of the electron in these systems. It can modify the electronic and the optical characteristics of the systems by altering the ILF parameter. In QW systems, linear and nonlinear transitions depending

on ILF have become an investigation matter in current years since they are not only physically appealing but also necessary in practice. Hopefully, our results will offer significant development of optical devices in many potential device applications for the appropriate selection of ILF values.

References

[1] Jiang X, Li S S and Tidrow M Z 1999 *Physica E* **5** 27
[2] Leobandung E, Guo L and Chou S 1995 *Appl. Phys. Lett.* **67** 2338
[3] Niculescu E, Radu A and Iorga A 2008 *University Politehnica of Bucharest Sci. Bull. Ser. A* **70** 51
[4] Ozturk E 2015 *Superlattices Microstruct.* **82** 303
[5] Phuc H V and Tung L V 2014 *Superlattices Microstruct.* **71** 124
[6] Karabulut I 2010 *Appl. Surf. Sci.* **256** 7570
[7] Ozturk E and Sokmen I 2012 *Opt. Commun.* **285** 5223
[8] Niculescu E C and Eseanu N 2011 *Eur. Phys. J. B* **79** 313
[9] Ozturk E 2010 *Eur. Phys. J. B* **75** 197
[10] Fulco U L, Albuquerque E L, Mauriz P W and Vasconcelos M S 2013 *Phys. Lett. A* **377** 582
[11] Unterrainer K, Heyman J N, Craig K, Galdrikian B, Sherwin M S, Campman K, Hopkins P F and Gossard A C 1996 *Semicond. Sci. Technol.* **11** 1591
[12] Vodopyanov K L, Chazapisdag V, Phillipsdag C, Sungddag B and HarrisJr J S 1997 *Semicond. Sci. Technol.* **12** 708
[13] Vodopyanov K L 2008 *Laser Photon. Rev.* **2** 11
[14] Zavvari M, Abedi K, Yusefli A and Karimi M 2015 *Optik* **126** 1861
[15] Zeiri N, Sfina N, Abdi-Ben Nasrallah S, Lazzari J L and Said M 2013 *Infrared Phys. Technol.* **60** 137
[16] Bhattacharya P and Mi Z 2007 *Proc. IEEE* **95** 1723
[17] Baskoutas S, Paspalakis E and Terzis A F 2007 *J. Phys.: Condens. Matter* **19** 395024
[18] Karimi M J and Keshavarz A 2012 *Physica E* **44** 1900
[19] Sakiroglu S, Ungan F, Yesilgul U, Mora-Ramos M E, Duque C A, Kasapoglu E, Sari H and Sokmen I 2012 *Phys. Lett. A* **376** 1875
[20] Aytekin O, Turgut S and Tomak M 2012 *Physica E* **44** 1612
[21] Xie W 2014 *J. Lumin.* **145** 283
[22] Martinez-Orozco J C, Mora-Ramos M E and Duque C A 2012 *J. Lumin.* **132** 449
[23] Liu X, Zou L, Liu C, Zhang Z H and Yuan J H 2016 *Opt. Mater.* **53** 218
[24] Restrepo R L, Gonzalez-Pereira J P, Kasapoglu E, Morales A L and Duque C A 2018 *Opt. Mater.* **86** 590
[25] Eseanu N, Niculescu E C and Burileanu L M 2009 *Physica E* **41** 1386
[26] Ozturk E 2016 *Opt. Quantum Electron.* **48** 269
[27] Lima F M S, Amato M A, Nunes O A C, Fonseca A L A, Enders B G and Silva Jr E F 2009 *J. Appl. Phys.* **105** 123111
[28] Kuech T F, Babcock S E and Mawst L 2016 *Appl. Phys. Rev.* **3** 040801
[29] Devenyi G A, Woo S Y, Ghanad-Tavakoli S, Hughes R A, Kleiman R N, Botton G A and Preston J S 2011 *J. Appl. Phys.* **110** 124316
[30] Owen J H G, Barvosa-Carter W and Zinck J J 2000 *Appl. Phys. Lett.* **76** 3070
[31] Mukai K, Sugawara M and Yamazaki S 1994 *Phys. Rev. B* **50** 2273
[32] Yuh P F and Wang K L 1989 *J. Appl. Phys.* **65** 4377
[33] Ozturk E 2015 *Eur. Phys. J. Plus* **130** 237
[34] Zhao G J, Liang X X and Ban S L 2003 *Phys. Lett. A* **319** 191
[35] Ozturk E and Sokmen I 2015 *Int. J. Mod. Phys. B* **29** 1550030
[36] Ozturk E 2014 *Opt. Commun.* **332** 136
[37] Peter A J and Navaneethakrishnan K 2008 *Superlattices Microstruct.* **43** 63
[38] Ozturk E and Sokmen I 2013 *J. Lumin.* **134** 42
[39] Pont M, Walet N R, Gavrila M and McCurdy C W 1988 *Phys. Rev. Lett.* **61** 939
[40] Niculescu E C 2017 *Opt. Mater.* **64** 540
[41] Zhang C 2001 *Appl. Phys. Lett.* **78** 4187
[42] Ozturk E 2016 *Laser Phys.* **26** 096102